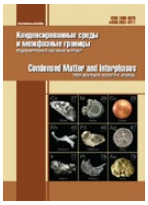

ISSN 1606-867X (Print)
ISSN 2687-0711 (Online)
Condensed Matter and Interphases
Kondensirovannye Sredy i Mezhfaznye Granitsy
https://journals.vsu.ru/kcmf/

Original articles

Research article
https://doi.org/10.17308/kcmf.2025.27/13023

Coupled effects of concentration polarization in systems with anion-exchange membranes before and after their participation in electrodialysis of tartrate-containing solutions

O. A. Yurchenko✉, K. V. Solonchenko, N. D. Pismenskaya

Kuban State Technological University
149 Stavropolskaya st., Krasnodar 350040, Russian Federation

Abstract

Objective: Homogeneous anion-exchange membranes ASE and heterogeneous anion-exchange membranes MA-41P were studied in 20±1 mM $NaxH_{(2-x)}T$ solutions with pH 2.5 and 9.0, where T is tartaric acid residue. Optical images and contact angles of membrane surfaces, as well as their current-voltage curves and pH of desalinated solutions, were measured before and after using ASE and MA-41P in electrodialysis.

Experimental results: The study determined that in alkaline solutions, the development patterns of concentration polarization do not differ from those of strong electrolytes. In acidic solutions, the ability of tartrates to participate in protonation-deprotonation reactions causes a 4-5 times increase in the empirical limiting current as compared to the theoretical limiting current calculated within the convective-diffusion model. The article discusses the mechanisms of tartrate transfer through anion-exchange membranes in cases when the desalinated solution contains mainly tartaric acid molecules.

Conclusions: Long-term operation (about 50 hours) under intensive current regimes results in the appearance of numerous caverns on the ASE surface and leads to an increase in the proportion of ion-exchange material on the MA-41P surface. The surfaces of both membranes become more hydrophobic. An analysis of current-voltage curves suggests that the electrochemical degradation of the ASE surface and specific interactions of tartrates with weakly basic fixed groups of both membranes lead to reduced proton generation and affect the development of electroconvection.

Keywords: Electrodialysis, Tartrates, Anion-exchange membranes, Current-voltage curves, Limiting current, Electroconvection, Catalytic water dissociation

Financing: The study was funded by the Russian Science Foundation and Kuban Science Foundation, project No. 24-29-20097

For citation: Yurchenko O. A., Solonchenko K. V., Pismanskaya N. D. Coupled effects of concentration polarization in systems with anion-exchange membranes before and after their participation in electrodialysis of tartrate-containing solutions. *Condensed Matter and Interphases*. 2025;27(3): 464–477. https://doi.org/10.17308/kcmf.2025.27/13023

Для цитирования: Юрченко О. А., Солонченко К. В., Письменская Н. Д. Сопряженные явления концентрационной поляризации в системах с анионообменными мембранами до и после их участия в электродиализе тартрат-содержащих растворов. *Конденсированные среды и межфазные границы*. 2025;27(3): 464–477. https://doi.org/10.17308/kcmf.2025.27/13023

✉ Olesya A. Yurchenko, olesia93rus@mail.ru

1. Introduction

Electrodialysis (ED) has been increasingly used for the extraction of tartaric acid from food industry waste for conversion of tartrate salts into tartaric acid [1], for the correction of pH of wine materials [2], and for the tartrate stabilization in wine [3]. Tartrate stabilization by means of electrodialysis involves removal of tartaric acid anions and potassium cations from the desalination chambers of electrodialyzers in applied electric field through anion-exchange membranes (AEM) and cation-exchange membranes (CEM) respectively. This helps to prevent tartrate precipitation during long-term wine storage [4–7]. Systematic studies of the application of electrodialysis in winemaking began in the 1970s [8, 9, 10] and resulted in the development of an automated technology [11, 12, 13] involving conventional membrane stacks with alternating cation and anion-exchange membranes [14] or a standard ED combined with bipolar membrane electrodialysis [15, 16]. The degree of wine demineralization in the desalination unit is controlled based on the electrical conductivity, which depends on the type of wine. A reduction in the electrical conductivity of wine by 20% corresponds to a 10–15% reduction in the concentration of tartaric acid. Exact parameters of ED for tartrate stabilization are usually determined specifically for each type of wine [17]. It is known that the optimal concentration of tartaric acid anions can be obtained, when the electrical conductivity is reduced by 15–20% for young wines, by 5–15% for aged wines [18], and by 20–30% for dessert wines [18, 19].

There are several factors that limit the widespread introduction of ED for the treatment of solutions with tartrates or various forms of other polybasic acids. One of the main drawbacks is low current efficiency and higher energy consumption as compared to those observed in the electrodialysis of strong electrolytes (for instance, NaCl) [20, 21]. Another drawback is the rapid degradation of the properties of anion-exchange membranes in solutions of polybasic acids and their salts [22, 23] as compared to strong electrolyte solutions. Both factors are associated with the structural features and the participation of polybasic acids in protonation-deprotonation reactions with water.

Tartaric acid (2,3-dihydroxybutanedioic acid, according to IUPAC, $C_4H_6O_6$) is a fairly large molecule containing two hydroxyl and two carboxyl groups (Fig. 1).

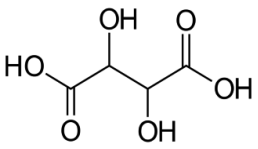

Fig. 1. Structural formula of tartaric acid [24]

The structure of tartaric acid (H_2T, where T is the acidic residue) results in a high degree of hydration of its anions (their hydration numbers are 14±3 [25]) and the possibility of steric hindrance during the transfer of these anions through an AEM [26]. There is also a possibility of specific interactions between carboxyl groups and primary and secondary amines, which are fixed groups in membranes. Such interactions, namely the formation of bound species, are characteristic for polybasic acids [27]. The binding behavior is caused by electrostatic interactions and the formation of hydrogen bonds, as well as by the donor-acceptor proton sharing between the carboxyl groups of acids and weakly basic amino groups [27]. The formation of bound species explains the sorption of polyvalent acid anions, including tartrates, by anion-exchange membranes described in a large number of studies [22, 23].

The protonation-deprotonation reactions, whose equilibrium constants can easily be found in reference literature [28], are described by the following equations:

$$C_4H_6O_6 + H_2O \leftrightarrow C_4H_5O_6^- + H_3O^+$$
$$K_1 = 1.12 \cdot 10^{-3}\ \text{mol/dm}^3 \quad (1)$$

$$C_4H_5O_6^- + H_2O \leftrightarrow C_4H_6O_6 + OH^- \quad (2)$$

$$C_4H_5O_6^- + H_2O \leftrightarrow C_4H_4O_6^{2-} + H_3O^+$$
$$K_2 = 5.62 \cdot 10^{-5}\ \text{mol/dm}^3 \quad (3)$$

$$C_4H_4O_6^{2-} + H_2O \leftrightarrow C_4H_5O_6^- + OH^- \quad (4)$$

Calculations based on these constants result in the distribution of molar fractions of various forms of tartaric acid depending on the pH of the solution (Fig. 2). These dependencies show that the electric charge of tartrates is extremely sensitive to the pH of the medium.

The purpose of our study was to perform a comparative analysis of the development of concentration polarization in anion-exchange

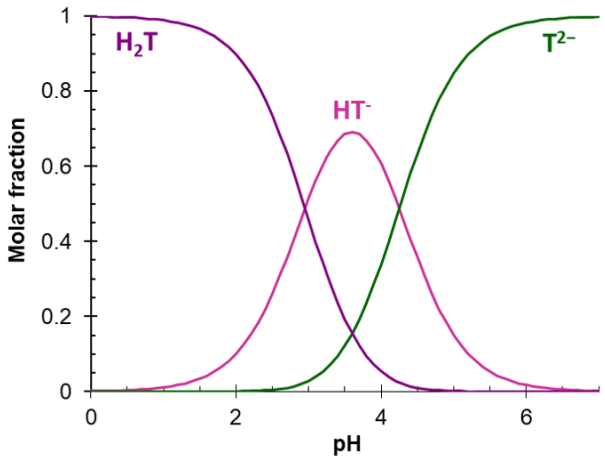

Fig. 2. Distribution of molar fractions of various forms of tartaric acid depending on the pH of the solution

membrane/$Na_xH_{(2-x)}T$ solution systems with a pH of 2.5 or 9.0 depending on the characteristics of the membrane surface, and to assess the impact of long-term membrane operation in these solutions on the process.

For this purpose we used an ASE homogeneous membrane (Astom, Japan) and an MA-41P heterogeneous membrane (LLC Shchekinoazot, Russia). The studies were performed using "fresh" membrane samples and samples that were employed in a laboratory ED unit during the extraction of tartrates from $Na_xH_{(2-x)}T$ solutions in underlimiting and overlimiting current modes.

2. Materials and methods

2.1. Solutions

Experiments were conducted in 20±1 mM $Na_xH_{(2-x)}T$ solutions prepared from tartaric acid powder (Vecton, Russia) and distilled water (resistance 1 MΩ·cm, pH 5.6±0.1). The pH values were adjusted using a 100±1 mM NaOH solution (Vecton, Russia). The total molar concentration of tartrates in the prepared solutions was determined using a DIONEX ICS-3000 chromatographic system (USA) with a conductometric detector and background signal suppression unit. The electrical conductivity of the solutions was measured at 25°C using an Expert-002 conductometer (OOO *Econix-Expert*, Russia). The distribution of various forms of tartaric acid depending on the pH of the solution was calculated taking into account the equilibrium constants of tartaric acid dissociation for the 1st and 2nd stages [28]. The main characteristics of the solutions are presented in Table 1.

2.2. Membranes

Some of the properties of anion-exchange membranes manufactured by Astom, Japan (ASE), and OOO *Shchekinoazot*, Russia (MA-41P) were described in previous articles [28, 29] and are summarized in Table 2. IR-Fourier spectroscopy [30] demonstrated that the ion-exchange material of a "fresh" pseudohomogeneous ASE membrane contains practically no weakly basic fixed groups. The electrochemical behavior of a heterogeneous MA-41P membrane in NaCl solutions also indicates the absence of such groups, at least previous to the operation of the membrane in intensive current modes [30]. The membranes are reinforced with nylon fabric (MA-41P) [31] or a mixture of polyethylene and polypropylene (ASE) [32]. The absence of macropores ensures a low volume fraction of intergel spaces (f_2) in the ASE membrane (Table 2). On the contrary, the MA-41P

Table 1. Some characteristics of the 20±1 mM $Na_xH_{(2-x)}T$ solution

pH	Electrical conductivity, μS·cm^{-1}	H_2T, %	HT^-, %	T^{2-}, %
2.5±0.1	1525±5	73.5±0.1	26.0±0.1	0.5±0.1
9.0±0.1	3570±5	0	0.1±0.1	99.9±0.1

Table 2. Some properties of the studied anion-exchange membranes

Membrane	Type	Ion-exchange matrix	Fixed groups	Q, mM·g_{wet}^{-1}*	f_2**	Θ***
ASE	homogeneous	PS+DVB	$-N^+(CH_3)_3$	1.93	0.06	1.0
MA-41P	heterogeneous			0.92	0.26	0.25

* Exchange capacity of the swollen membrane; determination error ± 0.05 mM·g_{wet}^{-1}
** Volume fraction of intergel spaces in NaCl solutions; determination error ± 0.02
*** Proportion of conductive surface; determination error ± 0.02
PS+DVB – polystyrene cross-linked with divinylbenzene

membrane is characterized by a rather high f_2 due to the presence of macropores between the threads of the reinforcing material and the ion-exchange composite, as well as between the inert binder and resin particles. Additionally, the AB-17-2 resin, which is part of MA-41P, contains only 2% of DVB.

Heterogeneous membranes MK-40 and MA-41 (OOO *Shchekinoazot*, Russia) are auxiliary. They contain sulfonate fixed groups (MK-40) and quaternary amines (MA-41). The characteristics of these membranes are detailed in [33, 34]. Prior to experiments, all the membranes underwent salt pretreatment [35]. They were then divided into 2 samples, each of which was equilibrated with a 20±1 mM $Na_xH_{(2-x)}T$ solution with pH 2.5 or 9.0.

2.3. Methods

The surface of swollen membranes was visualized using a SOPTOP CX40M optical microscope (Yuyao, Zhejiang, P.R., China). The MA-41P membrane was preliminarily soaked in a solution containing anthocyanins for 12 hours to increase the contrast of the anion-exchange resin particles on the surface of the inert binder – polyethylene.

Contact angles of the swollen membrane surfaces were measured using the sessile drop method as detailed in [36].

The current-voltage characteristics of the analyzed membranes were studied in a flow-through four-chamber electrodialysis cell described in [37]. The schematic diagram of the cell is shown in Fig. 1. One of the solutions presented in Table 1 was pumped through all the chambers of the ED cell. The average linear velocity of the solution in the chambers (V) was 0.40±0.01 cm·s^{-1}. The intermembrane distance (h), the length of the solution desalination path (L), and the polarized membrane area (S) were 6.6±0.1 mm, 20±1 mm, and 400±2 mm^2, respectively. Luggin capillaries were connected to the geometric centers of the surfaces of the studied anion-exchange membranes (*AEM). The distance between their tips and the surface was about 0.8 mm. The capillaries were connected to microchambers containing measurement Ag/AgCl electrodes EVL-1M3.1 (Gomel, Belarus). They in turn were connected to an Autolab PGSTAT-100 electrochemical station (Metrohm Autolab B.V., Kanaalweg, Netherlands). The same station was used to polarize the membrane stack of the ED cell through polarizing platinum electrodes. The current density scan rate was 2.3·10^{-3} mA cm^{-2}. Parallel to determining the current-voltage characteristics, the inlet and outlet pH in the desalination chamber was measured at regular intervals. To perform the measurements, combined electrodes were used, which were immersed in flow-through microchambers and connected to Expert-001 pH meters (OOO *Econix-Expert*, Russia).

All measurements were performed before and after electrodialysis desalination of 20±2 mM solutions of $Na_xH_{(2-x)}T$ with pH 2.5 or 9.0. During electrodialysis, the membranes functioned at current densities from 0 to 2.0 mA·cm^{-2} for 10 hours.

The reduced current-voltage characteristics (CVCs) were plotted in i – Δφ′ coordinates [38]. The reduced potential drop Δφ′ was determined based on the measured potential drops Δφ:

$$\Delta\varphi' = \Delta\varphi - IR_{ef}. \quad (5)$$

Here I is the applied current, R_{ef} is the effective ohmic resistance of the membrane and the solution located between the Luggin capillaries. It was determined based on the current-voltage characteristics as $d\varphi/dI$ where $I \to 0$.

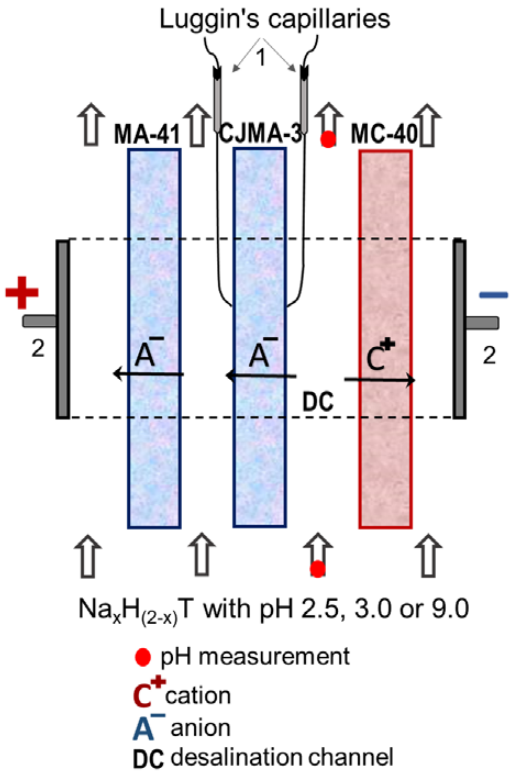

Fig. 3. Schematic diagram of the laboratory electrodialysis cell

The theoretical limiting current $i_{\text{lim}}^{\text{Lev}}$ was determined using the Levich equation derived within the framework of the convection-diffusion model [39]:

$$i_{\text{lim}}^{Lev} = \frac{z_1 F D c_1}{h(t_A - T_A)}\left[1.47\left(\frac{h^2 V_0}{LD}\right)^{1/3}\right]. \quad (6)$$

Here D is the diffusion coefficient of the electrolyte; z_1 and c_1 are the charge number and the concentration of the counterion (HT^- for the solution with pH 2.5 and T^{2-} for the solution with pH 9.0); t_A is the transport number of the co-ion (cation Na^+) during infinite dilution. The transport number T_A of the co-ion in the AEM was considered to be zero due to low electrolyte concentrations in the desalination and concentration chambers. For 20±1 mM solutions of $Na_xH_{(2-x)}T$ with pH 2.5 and 9.0 the calculated values of $i_{\text{lim}}^{\text{Lev}}$ were 0.56 and 4.10 mA cm^{-2} respectively.

3. Results and discussion

3.1. Optical images and contact angles of membrane surfaces

Fig. 4 shows optical images of the surfaces of the swollen membranes before and after ED.

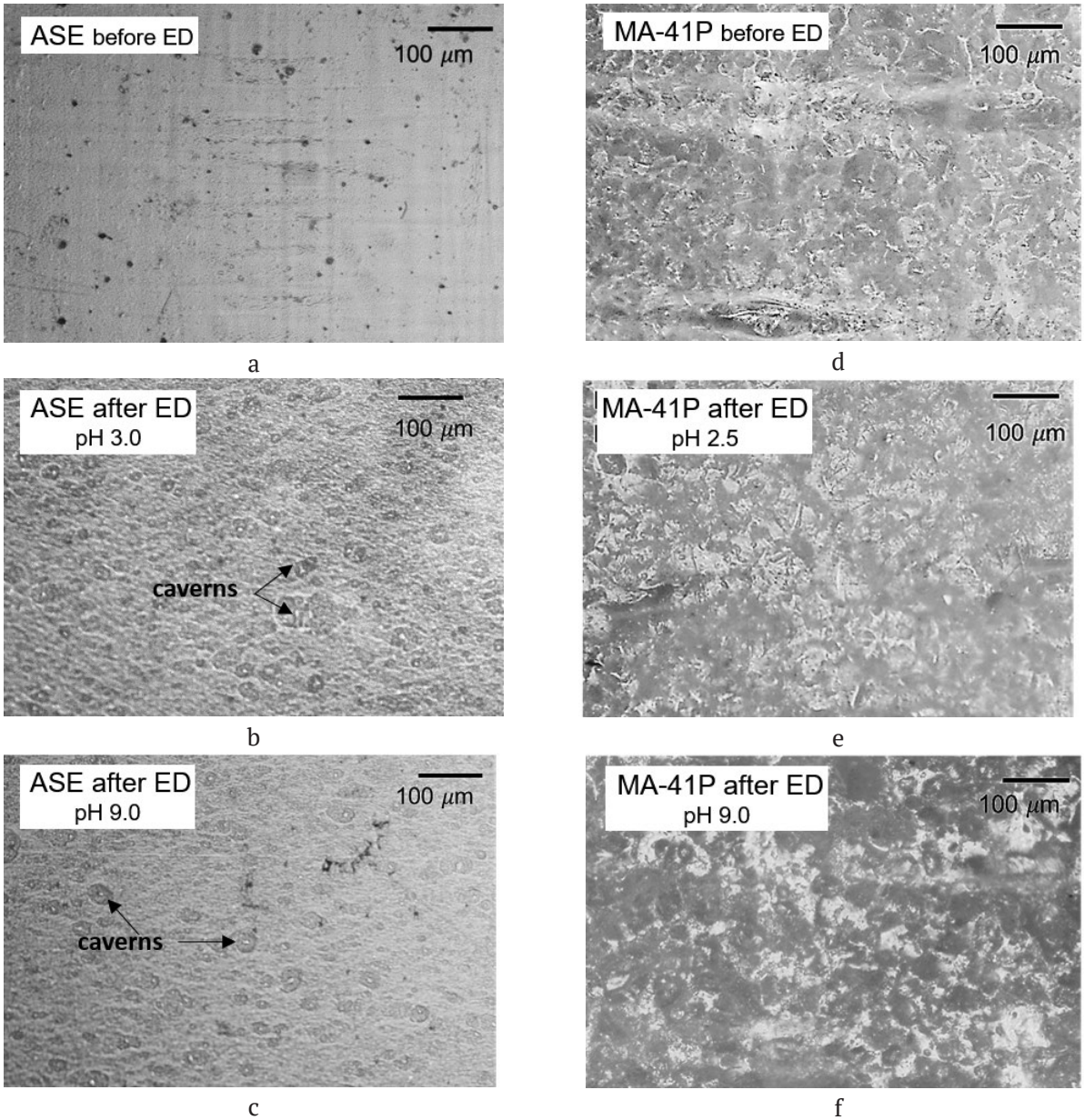

Fig. 4. Optical images of the surfaces of ASE (a, b, c) and MA-41P (d, e, f) membranes before and after ED

Table 3. Contact angles of membrane surfaces before and after their use for ED extraction of tartrates

Membrane	$Na_xH_{(2-x)}T$ with pH 2.5		$Na_xH_{(2-x)}T$ with pH 9.0	
	Before ED	After ED	Before ED	After ED
ASE	33±2°	31±3°	35±2°	45±3°
MA-41P	60±4°	69±2°	61±4°	68±2°

Table 3 presents the contact angles of the studied membrane surfaces before and after ED. During ED, these surfaces were facing the desalination chamber.

The surface of a "fresh" (not used in ED) ASE membrane was almost homogeneous (Fig. 4a). The ion-exchange material slightly protruded above the fibers of the reinforcing fabric. Other irregularities did not exceed a few micrometers. Apparently, the geometric heterogeneity is caused by the specifics of the pasting method of membrane manufacturing. The geometry of the ASE surface after ED underwent significant changes. Optical images (Fig. 4b, c) clearly demonstrate the appearance of caverns. They are evenly distributed over the membrane surfaces and reach several tens of μm in diameter. Moreover, when the membrane contacted the acidic solution (pH 2.5), the number of caverns increased compared to the alkaline solution (pH 9.0). The appearance of these caverns is no different from those observed on the surface of AMX and AMX-sb membranes [40] produced by Astom before switching to the production of ASE. This fact, as well as the results of IR spectroscopy [30], suggests that previously produced membranes (AMX) and new membranes (ASE) contain the same ion-exchange materials. It is these materials that undergo electrochemical destruction during membrane operation in intensive current modes. In other words, the use of a different inert binder and reinforcing material apparently did not help to reduce the electrochemical degradation of the ASE surface as compared to AMX during ED processing of tartrate-containing solutions.

The surface of a "fresh" heterogeneous MA-41P membrane consists of an inert binder (low-pressure polyethylene) and anion-exchange resin particles (Fig. 4d) and is rougher than the surface of a "fresh" ASE membrane. Threads of the reinforcing fabric were sometimes observed on the surface of MA-41P. No caverns identifiable by means of optical microscopy appeared after the use of the membrane in ED processing of tartrate-containing solutions (Fig. 4e, f). At the same time, the linear dimensions of the resin particles on the surface increased. A particularly noticeable increase in the linear dimensions and a 27% increase in the proportion of conductive surface as compared to a "fresh" membrane was observed after ED in $Na_xH_{(2-x)}T$ with pH 9.0. Apparently, changes in the linear dimensions of the resin particles (and MA-41P membranes) were caused by the factor we previously identified when studying MA-41 membranes kept in tartrate-containing solutions for a long time [41], namely the stretching of the ion-exchange matrix, when highly hydrated anions were introduced into its pores [25]. When an $Na_xH_{(2-x)}T$ solution with pH 2.5 is replaced with a solution with pH 9.0, the electric charge of tartaric acid anions increases. This should facilitate increased hydration and, respectively, result in an increase in the linear dimensions of the resin particles.

We should note that the use of ASE in a $Na_xH_{(2-x)}T$ solution with pH 2.5 does not result in any noticeable changes in the contact angle θ of the membrane surface as compared to "fresh" membranes (Table 3). When a solution with pH 9.0 was used, the increase in the contact angle of the ASE surface after ED significantly exceeded the measurement error. The surfaces of the MA-41P membrane became more hydrophobic after the ED of both acidic and alkaline solutions. The observed changes in the hydrophilic/hydrophobic balance were most likely caused by the loss of electrical charge by some fixed groups located on the surfaces of the studied membranes. We can assume that under intensive current modes, some of the quaternary amines transformed into weakly basic amino groups. This phenomenon was described in a number of studies, including [42]. In alkaline solutions, these groups were deprotonated and lost their electric charge [43]. In acidic solutions, they formed bound species

with HT^- anions, which have zero electric charge [30]. The hydrophilic/hydrophobic balance of the ASE membrane after ED in an acidic tartrate-containing solution is apparently affected by two opposing factors. On one hand, a decrease in the electric charge of the surface should contribute to an increase in the measured contact angle. On the other hand, an increase in the roughness parameters of the surface should result in a decrease in the contact angle [43], if the θ of the material does not exceed 90°.

3.2. Current-voltage characteristics of membranes and pH of desalinated solutions $Na_xH_{(2-x)}T$ with pH 9.0

Fig. 5 demonstrates the current-voltage characteristics of ASE and MA-41P membranes determined in a 20 mM $Na_xH_{(2-x)}T$ solution with pH 9.0, and the difference in the inlet and outlet pH in the desalination chamber of the laboratory electrodialyzer, measured in parallel to the measurement of the CVC. The data was

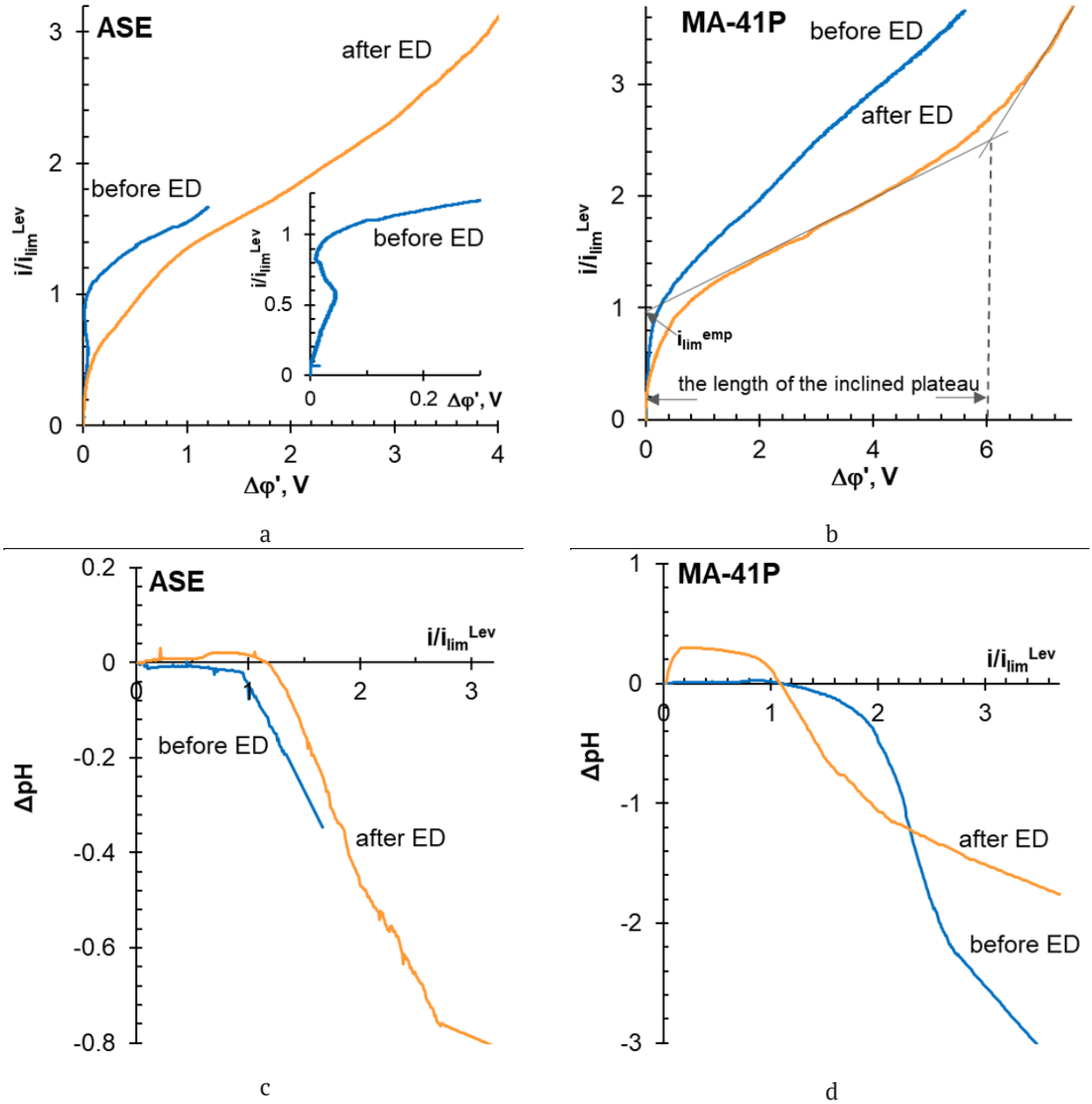

Fig. 5. Current-voltage characteristics of ASE (a) and MA-41P (b) membranes obtained in a 20 mM $Na_xH_{(2-x)}T$ solution with pH 9.0, and the difference between the inlet and outlet pH in the desalination channel of the laboratory electrodialyzer, measured in parallel with obtaining the CVCs of ASE (c) and MA-41P (d) membranes. Explanations are provided in the text

obtained using "fresh" membranes (before ED) and membranes used for the ED processing of the said solutions (after ED). The results of the graphical processing of the CVC are summarized in Table 4. The empirical limiting current i_{lim}^{emp} and the length of the inclined plateau in the CVC were determined as shown in Fig. 5b.

We should note that the $Na_xH_{(2-x)}T$ solution with pH 9.0 contains only trace amounts of HT^- anions and almost 100% of T^{2-} anions (Fig. 2, Table 1). Due to the Donnan exclusion of protons formed as a result of autoprotolysis of water, the pH of the internal solution of the AEM was higher than that of the external solution. In this case, T^{2-} anions in both the membrane and the depleted solution did not undergo any changes. Therefore, the mechanism of their transfer (Fig. 6a) and development of concentration polarization were the same as observed in strong electrolytes.

Increased current density causes a gradual decrease in the concentration of the electrolyte (Na_2T) in the depleted solution near the membrane surface. The decrease results from the diffusion limitations for the transport of the electrolyte to the AEM interface. A limiting state is formed, when the concentration of Na_2T in the solution near the interphase region is infinitely low as compared to that in the depth of the solution in the desalination chamber. This state corresponds to i_{lim}^{Lev}, determined within the framework of the convection-diffusion model using equation (4). For fresh ASE membranes, i_{lim}^{emp} exceeds i_{lim}^{Lev} by 18% (Fig. 5a, Table 4), and the initial section of CVC demonstrates a characteristic decrease in conductivity (insertion in Fig. 5a). This indicates the presence of the Dukhin–Mishchuk electroconvection near the ASE surface, which develops in a thresholdless manner [44, 45]. Slight electroconvective vortices transport the more concentrated solution to the surface, thus shifting the formation of the limiting state (i_{lim}^{emp}) towards the region of higher current densities. At

Table 4. Values of empirical limiting currents and lengths of the inclined plateau section found by means of graphical processing of CVCs

pH of $Na_xH_{(2-x)}T$	Parameter	ASE		MA-41P	
		Before ED	After ED	Before ED	After ED
9.0	$i_{lim}^{emp}/i_{lim}^{Lev*}$	1.18	0.98	1.08	0.95
	length of plateau, V	1.09	3.30	2.09	6.01
2.5	$i_{lim}^{emp}/i_{lim}^{Lev}$	3.55	4.13	4.95	3.56
	length of plateau, V	0.56	1.24	2.14	2.63

* The error in determining i_{lim}^{emp} is ±3 %

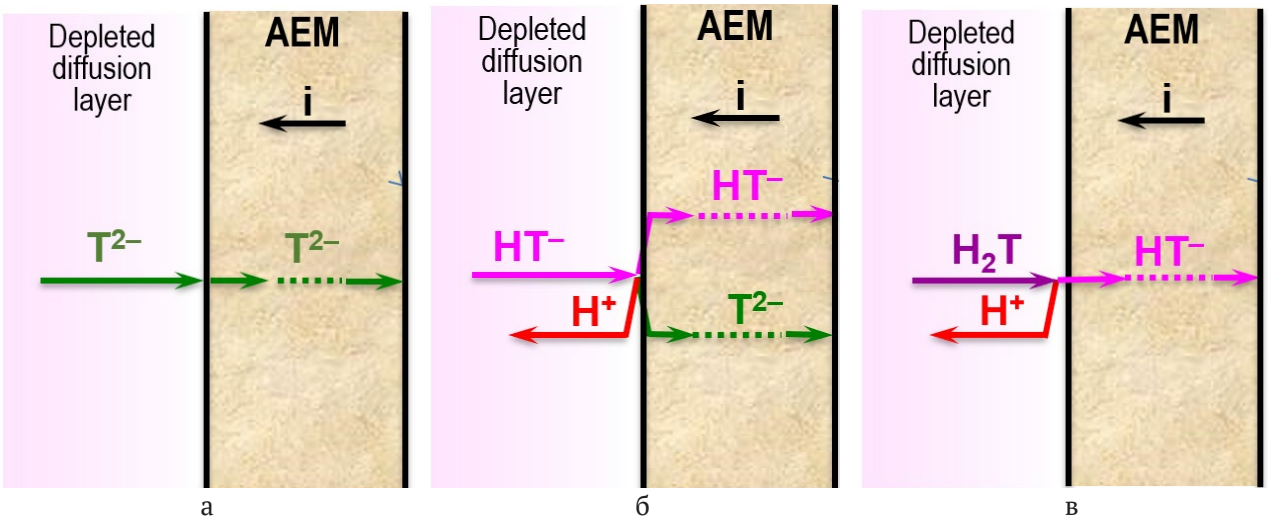

а б в

Fig. 6. Schematic representation of the transport mechanisms of anions T^{2-} (a), HT^- (b) and H_2T (c) in anion-exchange membrane and adjacent depleted solution in an applied electric field

higher current densities, the shortage of charge carriers in the near-membrane depleted solution result in a rapid potential drop (the region of the inclined plateau in the CVC). It is known that the slope of the CVC plateau can be accounted for by catalytic water dissociation (CWD) with the participation of fixed membrane groups and Rubinstein–Zaltzman electroconvection [46, 47]. Both processes develop in the threshold mode. According to [38], for the feed solutions with the concentration of electrolyte of 20 mM, the critical reduced potential drop for the onset of CWD is 0.3 V.

Indeed, after reaching this value, acidification of the desalinated solution was observed (Fig. 5c), which increased with an increase in the applied current. Despite the constant influx of protons, formed as a result of CWD, into the near-membrane solution, after reaching the threshold value of $\Delta\varphi'$ equal to the length of the inclined plateau, potential drop did not significantly grow with an increase in the current density. This overlimiting section of the CVC corresponds to the formation of large clusters of EC vortices in accordance with the Rubinstein–Zaltzman mechanism [47, 48].

For the MA-41P membrane (Fig. 5b), the concentration polarization developed in a similar way. The difference in the process, as compared to the ASE membrane, was caused by both electrical and geometric heterogeneity of the MA-41P surface. In our previous studies [31] we demonstrated that the heterogeneity parameters of this membrane are optimal for the development of both types of electroconvection. Therefore, with only 25% of the conductive surface, MA-41P demonstrated $i_{\text{lim}}^{\text{emp}}$ equal to $i_{\text{lim}}^{\text{Lev}}$, within the limits of measurement error. Similar to ASE, catalytic water dissociation begins at critical values of the reduced potential drop (Fig. 5d). However, the intensive delivery of the electrolyte by clusters of EC vortices to the MA-41P surface shifted the intense acidification of the desalinated solution towards the region of higher $i/i_{\text{lim}}^{\text{Lev}}$. Provided that all other conditions were equal, local current density values in the area of anion-exchange resin particles on the MA-41P surface were higher than those of the ASE. Therefore, the desalinated solution became more acidic, and the recorded reduced potential drops had higher values for the heterogeneous membrane as compared to the homogeneous one [31].

After the ED processing of the $Na_xH_{(2-x)}T$ solution with pH 9.0, the empirical limiting current decreased by 17%, while the length of the inclined plateau increased by 3.0 times for the ASE membrane as compared to the fresh sample. For the MA-41P membrane, these parameters were 12% and 3.0 times, respectively (Fig. 5a, b, Table 4). The difference between the inlet and outlet pH in the desalination channel decreased for both studied membranes (Fig. 5d, e). The causes of these changes have already been discussed in section 3.1. On one hand, specific interactions of tartrates with weakly basic fixed groups on the membrane surface weakened the influence of these catalytically active groups (primary and secondary amines) on the generation of H^+ and OH^- ions. On the other hand, these interactions apparently led to a decrease in the electric charge of the surface. This, in turn, resulted in a weakening of electroconvection developed in accordance with the Dukhin–Mishchuk mode. The weakening of this type of electroconvection is most obvious in the CVC of the ASE membrane used in ED. We should note that the CVC of a fresh membrane contained a section where the value of the reduced potential drop decreased as compared to that reached at $i \approx 0.5 i_{\text{lim}}^{\text{Lev}}$ (Fig. 5a). The CVC of the same membrane after ED demonstrated only a slowdown in the growth of $\Delta\varphi'$ at $0.6 i_{\text{lim}}^{\text{Lev}} < i < 1.1 i_{\text{lim}}^{\text{Lev}}$.

Apparently, changes in the surface charge negatively affect the space charge density, which determined the degree of development of Rubinstein-Zaltzman electroconvection. As a result, the threshold potential drops at which individual EC vortices merge into large clusters are shifted towards the region of higher $\Delta\varphi'$. Moreover, for both membranes, the "lengthening" of the inclined plateau, which is an indicator of this phenomenon, takes place despite the fact that the hydrophobicity of the ASE and MA-41P surfaces increased after ED. In other words, facilitating the slip of EC vortices along the membrane surface had less influence on the degree of electroconvection development than changes in the structure of the double electric layer and the space charge region, which was caused by specific interactions of tartrates with fixed groups on the membrane surface.

$Na_xH_{(2-x)}T$ with pH 2.5

Current-voltage characteristics of ASE and MA-41P membranes obtained in a 20 mM $Na_xH_{(2-x)}T$ solution with pH 2.5 are presented in Fig. 7. The results of their graphical processing are summarized in Table 4. Changes in the pH of desalinated solutions caused by phenomena developing at the AEM/depleted solution interface appear to be insignificant, considering a fairly high concentration of protons in the core of the flow. They cannot be recorded on the ΔpH – *i* dependencies. Therefore, we are not going to discuss these dependencies.

Note that the feed $Na_xH_{(2-x)}T$ solution with pH 2.5 contained only 26.5% of tartrate anions. These were mostly HT^- anions. The other tartrates are located in tartaric acid molecules, which should not participate in electric charge transfer. The fact that for fresh membranes, the values of i_{lim}^{emp} exceed the values of i_{lim}^{Lev} by 3.55 (ASE) and 4.95 (MA-41P) times indicates the presence of mass transfer caused by the participation of various forms of tartaric acid in the protonation-deprotonation reactions. Indeed, the effect of these reactions on the transfer of HT^- anions has been studied both by means of experimental methods and mathematical modelling. These results are summarized in [38], and the mechanism of transfer, called acid dissociation (AD), is schematically presented in Fig. 6b. HT^- anions participate in protonation-deprotonation reactions in accordance with equations (1) and (2) presented in the introduction. These reactions occurred both in solutions and in AEMs. At the same time, the Donnan exclusion of co-ions took place in the AEM [48]. Therefore, protons, which are one of the products of reactions (1), (3), were excluded from the membrane, and the AEM was enriched with doubly charged T^{2-} anions. Doubling the electric charge of counterions in the membrane and the constant influx of protons into the near-membrane depleted solution resulted in an increase in current density without a significant increase in the potential drop. Δφ′ began to grow only when the AEM was saturated with T^{2-} anions. In this case, the rate of proton influx into the depleted solution ceased to increase with increased current density. Therefore, the incoming protons could not compensate for the increase in the resistance of the near-membrane solution, which was caused by diffusion limitations of counterion (HT^-) delivery from the depth of the desalinated solution to the membrane surface. Theoretical estimates demonstrate that at the maximum possible concentration of monovalent anions in the feed solution, which corresponds to pH 3.6 (Fig. 1), we can expect an increase in i_{lim}^{emp} by 2.2 times

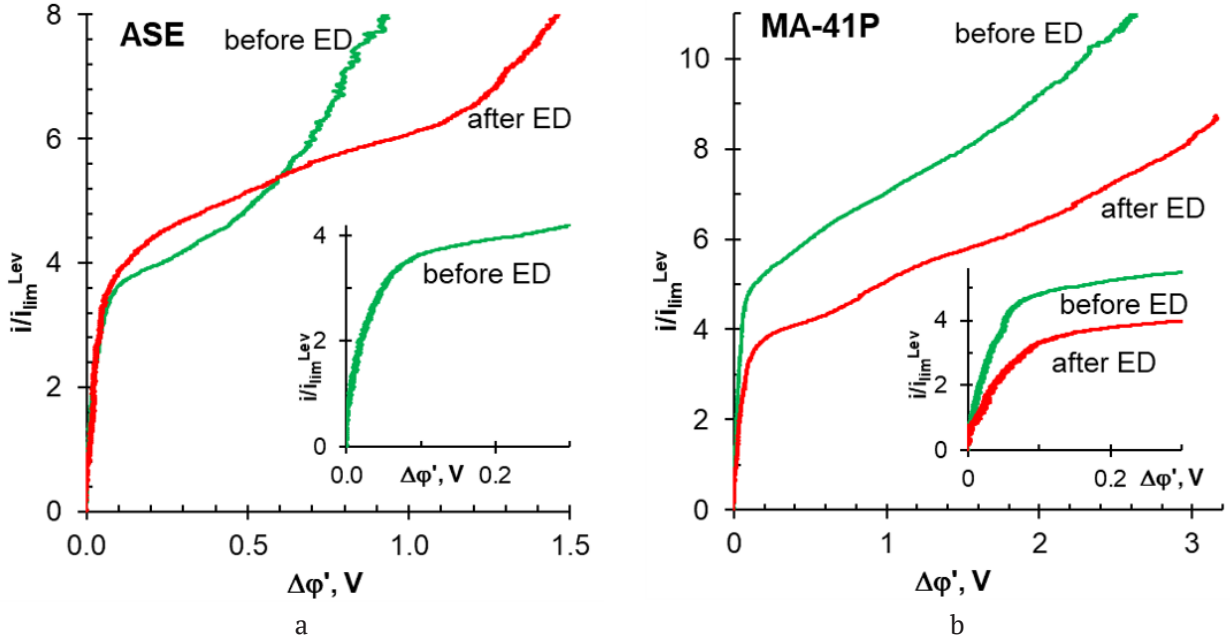

Fig. 7. Current-voltage characteristics of ASE (a) and MA-41P (b) membranes obtained in a 20 mM $Na_xH_{(2-x)}T$ solution with pH 2.5. Explanations are provided in the text

as compared to the limiting current i_{lim}^{Lev}. Higher values of recorded empirical limiting currents (Fig. 7, Table 4) indicate the anions initially contained in the feed solution were not the only ones being transferred through anion-exchange membranes. The source of additional HT^- anions were, apparently, tartaric acid molecules located in the near-membrane depleted solution. By analogy with the results of mathematical modelling [49] and the experimental study [50] of the transfer of weak acetic acid in membrane systems, the following scheme can be suggested (Fig. 6c). The dissociation of H_2T near the AEM surface is stimulated by the constant removal of resulting protons and HT^- anions from the reaction zone caused by an external electric field. Based on the results of mathematical modelling [50], we can expect that the degree of H_2T dissociation will be higher, when the tartaric acid molecules are closer to the AEM surface and at higher values of the applied current density. A similar hypothesis was suggested by Martí-Calatayud et al. [51]. They performed ED separation of citric acid and nitrate anions and observed the enhanced transfer of citrates through the AEM as the number of nitrates in the desalinated solution decreased. Apparently, HT^- anions are the first to be transferred from the feed depleted solution into the AEM. As charge carriers in the near-membrane solution are depleted, irreversible acid dissociation intensifies near the AEM surface. The observed values of i_{lim}^{emp} can be explained by at least two factors: the values of the kinetic constants of tartaric acid protonation-deprotonation reactions and the rate of H_2T molecule delivery from the depth of the solution to the AEM/depleted solution interface. Kinetic constants depend on the values of the equilibrium constants of acid dissociation for the first and second stages and on the rate of product removal from the reaction zone. The rate of H_2T molecule delivery to the AEM boundary will depend on the solution flow rate in the desalination chamber (thickness of the depleted diffusion layer), as well as on the degree of electroconvection development according to the Dukhin-Mishchuk mode. The characteristics of the MA-41P surface are more favorable for the development of this type of EC [31] than the ASE. The fact that for MA-41P the recorded values of i_{lim}^{emp} of a fresh membrane were higher than for ASE suggests that under the conditions of the experiment, electroconvective delivery of acid to the AEM surface is crucial. Unfortunately, in acidic solutions, the influence of Dukhin–Mishchuk EC on the CVC shape is masked by the influx of protons into the depleted solution, which are generated by the AD mechanism (insets in Fig. 7). Therefore, this hypothesis needs to be further verified by means of mathematical modelling.

We should note that the length of the inclined plateau on the CVCs obtained for the solution with pH 2.5 for fresh ASE and MA-41P membranes decreased by almost 2 times as compared to the solution with pH 9.0. Intense oscillations of the potential drop in the overlimiting section of the CVC indicate the formation of EC vortex clusters according to the Rubinstein-Zaltzman mechanism. The causes of the intensification of this type of electroconvection in acidic solutions are not yet fully clear.

Long-term operation of membranes during the electrodialytic processing of $Na_xH_{(2-x)}T$ solution with pH 2.5 had a different effect on the CVCs of the studied membranes. When the ASE membrane was used, the empirical limiting current increased by 16%, and the length of the inclined plateau increased by 2.2 times as compared to the fresh sample. The behavior of the MA-41P membrane after ED was different. The empirical limiting current decreased by 28%, and the length of the inclined plateau increased only by 20%.

The increase in i_{lim}^{emp} in the case of ASE could be facilitated by Dukhin–Mishchuk EC. Its enhancement is most likely caused by the appearance of numerous caverns on the surface of the membrane after ED. A similar effect was observed in the case of long-term operation of AMX and AMX-sb membranes [41], which were taken out of production and replaced with ASE [52]. It is known [46], that excessive development of the Dukhin-Mishchuk EC can shift the Rubinstein–Zaltzman formation of EC vortex clusters towards the region of higher potentials. This is apparently what happened in the case of the ASE membrane. Noticeable hydrophobization of the MA-41P surface (Table 4) is an indicator of partial loss of electric charge by its fixed

groups. Apparently, the change in the structure of the double electric layer caused a weakening of the Dukhin–Mishchuk EC and reduced the number of tartaric acid molecules delivered to the conductive surface of this membrane.

4. Conclusions

Voltammetry combined with optical visualization and measurement of contact angles of swollen membrane surfaces is a highly informative method for studying mass transfer mechanisms of various forms of tartaric acid.

When the feed solution $Na_xH_{(2-x)}T$ (T is the tartaric acid residue) contains mainly doubly charged T^{2-} anions, the mechanisms of transfer of these ions through anion-exchange membranes (AEM) do not differ from the well-known mechanisms of strong electrolyte transfer. The presence of geometric heterogeneity and high electric charge of the homogeneous membrane surface (ASE, Astom, Japan) or optimal parameters of electrical heterogeneity of the heterogeneous membrane (MA-41P, OOO *Shchekinoazot*) stimulate electroconvection and overlimiting mass transfer.

When the feed solution $Na_xH_{(2-x)}T$ contains 26.5% of anions and 73.5% of acid molecules, the mechanisms of tartrate transfer in membrane systems become more complex. Regardless of the properties of AEM surfaces, the empirical limiting currents i_{lim}^{emp}, which are determined by means of graphical processing of current-voltage characteristics, appear to be several times higher than those that could be caused by the transfer of tartrate anions present in the feed solution. The observed increase in i_{lim}^{emp} can be caused by the irreversible dissociation of tartaric acid in the depleted solution near the AEM surface. It results form the continuous removal of protons and HT^- anions from the reaction zone in the applied electric field.

Long-term participation in the electrodialytic processing of $Na_xH_{(2-x)}T$ solutions with pH 2.5 or 9.0 affects the hydrophilic/hydrophobic balance and morphology of ASE and MA-41P surfaces, as well as the degree of electroconvection development in the depleted solution adjacent to them. The dependence of i_{lim}^{emp} registered in acidic solutions on the conditions affecting the development of electroconvection suggests that irreversible dissociation of tartaric acid is limited by its delivery to the anion-exchange membrane surface.

Author contributions

Yurchenko O. A. – research hypothesis, text writing, final conclusions. Solonchenko K. V. – selection and systematization of material, conducting research, text editing. Pismenskaya N. D. – text writing, research concept, final conclusions.

Conflict of interests

The authors declare that they have no known competing financial interests or personal relationships that could have influenced the work reported in this paper.

References

1. Andrés L. J., Riera F. A., Alvarez R. Recovery and concentration by electrodialysis of tartaric acid from fruit juice industries waste waters. *Journal of Chemical Technology and Biotechnology*. 1997;70(3): 247–252. https://doi.org/10.1002/(sici)1097-4660(199711)70:3<247::aid-jctb763>3.0.co;2-8

2. Ioannidou S. M., Filippi K., Kookos I. K., Koutinas A., Ladakis D. Techno-economic evaluation and life cycle assessment of a biorefinery using winery waste streams for the production of succinic acid and value-added co-products. *Bioresource Technology*. 2022;348: 126295. https://doi.org/10.1016/j.biortech.2021.126295

3. Ncube A., Fiorentino G., Colella M., Ulgiati S. Upgrading wineries to biorefineries within a Circular Economy perspective: An Italian case study. *Science of the Total Environment*. 2021;775: 145809. https://doi.org/10.1016/j.scitotenv.2021.145809

4. Liu G., Wu D., Chen G., Halim R., Liu J., Deng H. Comparative study on tartaric acid production by two-chamber and three-chamber electro-electrodialysis. *Separation and Purification Technology*. 2021;263: 118403. https://doi.org/10.1016/j.seppur.2021.118403

5. El Rayess Y., Castro-Muñoz R., Cassano A. Current advances in membrane processing of wines: A comprehensive review. *Trends in Food Science and Technology*. 2024;147: 104453. https://doi.org/10.1016/j.tifs.2024.104453

6. Cabrita M. J., Garcia R., Catarino S. *Recent developments in wine tartaric stabilization*. Recent Advances in Wine Stabilization and Conservation Technologies. New York: Nova Publishers; 2016. Режим доступа: http://hdl.handle.net/10174/19263

7. Thoukis G. *Chemistry of wine stabilization: a review*. Washington: Chemistry of Wine Making, American Chemical Society; 1974. Режим доступа: http://jkliks.prv.pl/1.pdf

8. Audinos R., Roson J. P., Jouret C. Application de l'électrodialyse à l'élimination de certains composants du jus de raisin et du vin essais de laboratoire. *OENO One Vin*. 1979;13: 229–239. https://doi.org/10.20870/oeno-one.1979.13.3.1402

9. Paronetto L., Braido A. *Some tests on tartrate stabilization of musts and wines by electrodialysis*. Vignevini. 1977;4:

9–15. Режим доступа: https://agris.fao.org/search/en/providers/123819/records/64735a0753aa8c896307d146

10. Wucherpfennig K. Stabilization of grape juice and wine against tartar by means of electrodialysis. In: *Proceedings of the International Symposium on Separation Processes "Membr. Ion-Exch. Freeze-Cone. Food Ind." A.P.R.I.A., Paris*; 1975. 5-9.

11. Escudier J. L. Stabilisation tartrique des vins par membranes: resultats et developments technologiques. In: *Proceedings of 11 eme Colloque Viticole et Oenologique Montpellier, France*; 1997.

12. Moutounet M., Escudier J.-L., Saint-Pierre B. In: *Les Acquisitions R´ecentes dans les Traitements Physiques du Vin (ed. B. Don`eche)*. Paris: Tec. et Doc., Lavoisier. 1994. Режим доступа: https://www.researchgate.net/profile/Jean-Louis-Escudier-2/publication/304496184_Determination_du_degre_d'instabilite_tartrique_DIT_principes_et_applications/links/6570e65ad21eb37cd4fa251d/Determination-du-degre-dinstabilite-tartrique-DIT-principes-et-applications?__cf_chl_tk=5z9Ff3qrXe_gnwCwDxESImpb5Zas.oJ1GrbxdZc92I8-1733311140-1.0.1.1-XOzdBDi8lnhM m0ht2lVWq1SshEy93 VpyvVInJYRXZ2c

13. Wollan D. Membrane and other techniques for the management of wine composition. *Managing Wine Quality*: 2021: 183–212. https://doi.org/10.1016/b978-0-08-102065-4.00032-8

14. Gonçalves F., Fernandes C., Cameira dos Santos P., De Pinho M. N.Wine tartaric stabilization by electrodialysis and its assessment by the saturation temperature. *Journal of Food Engineering*. 2003;59(2-3): 229–235. https://doi.org/10.1016/s0260-8774(02)00462-4

15. El Rayess Y., Achcouty S., Ghanem C., Rizk Z., Nehme N. *Clarification and stabilization of wines using membrane processes.* In: Recent advances in wine stabilization and conservation technologies. NY, USA, Hauppauge: Nova Science Publishers; 2016: 111–135.

16. Vecino X., Reig M., Gibert O., Valderrama C., Cortina J. L. Integration of monopolar and bipolar electrodialysis processes for tartaric acid recovery from residues of the winery industry. *ACS Sustainable Chemistry and Engineering*. 2020;8(35): 13387–13399. https://doi.org/10.1021/acssuschemeng.0c04166

17. Soares P. A. M. H., Geraldes V., Fernandes C., Dos Santos P. C., De Pinho M. N. Wine tartaric stabilization by electrodialysis: prediction of required deionization degree. *American Journal of Enology and Viticulture*. 2020;60(2): 183–188. https://doi.org/10.5344/ajev.2009.60.2.183

18. Ribéreau-Gayon P., Glories Y., Maujean A., Dubourdieu D. *Handbook of enology: the chemistry of wine, stabilization and treatments*. 2nd ed. Volume 2: Dunod, Paris. 2006.

19. Gómez Benítez J., Palacios Macías V. M., Szekely Gorostiaga P., Veas López R., Pérez Rodríguez L. Comparison of electrodialysis and cold treatment on an industrial scale for tartrate stabilization of sherry wines. *Journal of Food Engineering*. 2003;58(4): 373–378. https://doi.org/10.1016/s0260-8774(02)00421-1

20. Fidaleo M., Ventriglia G. Application of design of experiments to the analysis of fruit juice deacidification using electrodialysis with monopolar membranes. *Foods*. 2022;11(12): 1770. https://doi.org/10.3390/foods11121770

21. Liu G., Wu D., Chen G., Halim R., Liu J., Deng H. Comparative study on tartaric acid production by two-chamber and three-chamber electro-electrodialysis. *Separation and Purification Technology*. 2021;263: 118403. https://doi.org/10.1016/j.seppur.2021.118403

22. Zhang Y., Pinoy L., Meesschaert B., Van der Bruggen B. Separation of small organic ions from salts by ion-exchange membrane in electrodialysis. *AIChE Journal*. 2011;57(8): 2070–2078. https://doi.org/10.1002/aic.12433

23. Chandra A., Chattopadhyay S. Chain length and acidity of carboxylic acids influencing adsorption/desorption mechanism and kinetics over anion exchange membrane. *Colloids and Surfaces A: Physicochemical and Engineering Aspects*. 2020;589: 124395. https://doi.org/10.1016/j.colsurfa.2019.124395

24. Koga Y., Kondo T., Miyazaki Y., Inaba A. The effects of sulphate and tartrate ions on the molecular organization of water: towards understanding the Hofmeister series (VI). *Journal of Solution Chemistry*. 2012;41: 1388–1400. https://doi.org/10.1007/s10953-012-9880-x

25. Chandra A., Bhuvanesh E., Chattopadhyay S. A critical analysis on ion transport of organic acid mixture through an anion-exchange membrane during electrodialysis. *Chemical Engineering Research and Design*. 2022;178: 13–24. https://doi.org/10.1016/j.cherd.2021.11.035

26. Laucirica G., Pérez-Mitta G., Toimil-Molares M. E., Trautmann C., Marmisollé W. A., Azzaroni O. Amine-phosphate specific interactions within nanochannels: binding behavior and nanoconfinement effects. *The Journal of Physical Chemistry C*. 2019;123(47): 28997–29007. https://doi.org/10.1021/acs.jpcc.9b07977

27. Lide D. R. *CRC handbook of chemistry and physics* (Vol. 85). CRC Press; 2004.

28. Sugimoto Y., Ujike R., Higa M., Kakihana Y., Higa M. Power generation performance of reverse electrodialysis (RED) using various ion exchange membranes and power output prediction for a large RED stack. *Membranes*. 2022;12: 1141. https://doi.org/10.3390/membranes12111141

29. Pismenskaya N., Rybalkina O., Solonchenko K., Pasechnaya E., ... Nikonenko V. How chemical nature of fixed groups of anion-exchange membranes affects the performance of electrodialysis of phosphate-containing solutions? *Polymers*. 2023;15(10): 2288. https://doi.org/10.3390/polym15102288

30. Pismenskaya N.D., Pokhidnia E.V., Pourcelly G., Nikonenko V.V. Can the electrochemical performance of heterogeneous ion-exchange membranes be better than that of homogeneous membranes? *Journal of Membrane Science.* 2018;566: 54–68. https://doi.org/10.1016/j.memsci.2018.08.055

31. *Monopolar membranes*. Available at: http://azotom.ru/monopolyarnye-membrany/

32. Chen G. Q., Wei K., Hassanvand A., Freeman B. D., Kentish S. E. Single and binary ion sorption equilibria of monovalent and divalent ions in commercial ion exchange membranes. *Water Research*. 2020;175: 115681. https://doi.org/10.1016/j.watres.2020.115681

33. Kozaderova O. A., Kim K. B., Gadzhiyeva C. S., Niftaliev S. I. Electrochemical characteristics of thin heterogeneous ion exchange membranes. *Journal of Membrane Science*. 2020;604: 118081. https://doi.org/10.1016/j.memsci.2020.118081

34. Vasilyeva V. I., Meshcheryakova E. E., Falina I. V., Kononenko N. A., Brovkina M. A., Akberova E. M. Effect of

Heterogeneous Ion-Exchange Membranes Composition on Their Structure and Transport Properties. *Membranes and Membrane Technologies*. 2023;13(3): 163–171. https://doi.org/10.31857/S2218117223030082

35. Berezina N. P., Timofeev S. V., Kononenko N. A. Effect of conditioning techniques of perfluorinated sulphocationic membranes on their hydrophylic and electrotransport properties. *Journal of Membrane Science*. 2002;209(2): 509–518. https://doi.org/10.1016/S0376-7388(02)00368-X

36. Ponomar M., Krasnyuk E., Butylskii D., ... Pismenskaya N. Sessile drop method: critical analysis and optimization for measuring the contact angle of an ion-exchange membrane surface. *Membranes*. 2022;12: 765. https://doi.org/10.3390/membranes12080765

37. Rybalkina O. A., Sharafan M. V., Nikonenko V. V., Pismenskaya N. D. Two mechanisms of H+/OH− ion generation in anion-exchange membrane systems with polybasic acid salt solutions. *Journal of Membrane Science*. 2022;651: 120449. https://doi.org/10.1016/j.memsci.2022.120449

38. Maletzki F., Rösler H. W., Staude E. Ion transfer across electrodialysis membranes in the overlimiting current range: stationary voltage current characteristics and current noise power spectra under different conditions of free convection. *Journal of Membrane Science*. 1992;71(1-2): 105–116. https://doi.org/10.1016/0376-7388(92)85010-G

39. Lévêque M. A. *The laws of heat transmission by convection*. Les Annales des Mines: Memoires. 1928;12(13). 201–299.

40. Rybalkina O. A., Tsygurina K. A., Sarapulova V.V., Mareev S.A., Nikonenko V.V., Pismenskaya N. D. Evolution of current-voltage characteristics and surface morphology of homogeneous anion-exchange membranes during the electrodialysis desalination of alkali metal salt solutions. *Membranes and Membrane Technologies*. 2019;9(2): 131–145. https://doi.org/10.1134/S2218117219020093

41. Pismenskaya N., Sarapulova V., Nevakshenova E., Kononenko N., Fomenko M., Nikonenko V. Concentration dependencies of diffusion permeability of anion-exchange membranes in sodium hydrogen carbonate, monosodium phosphate, and potassium hydrogen tartrate solutions. *Membranes*. 2019;9(12): 170. https://doi.org/10.3390/membranes9120170

42. Zabolotskii V. I., Chermit R. K., Sharafan M. V. Mass transfer mechanism and chemical stability of strongly basic anion-exchange membranes under overlimiting current conditions. *Russian Journal of Electrochemistry*. 2014;50(1): 45. https://doi.org/10.7868/S0424857014010113

43. Quéré D. Rough ideas on wetting. *Physica A: Statistical Mechanics and its Applications*. 20022;313(1-2): 32–46. https://doi.org/10.1016/s0378-4371(02)01033-6

44. Dukhin S. S. Electrokinetic phenomena of the second kind and their applications. *Advances in Colloid and Interface Science*. 1991;35: 173–196. https://doi.org/10.1016/0001-8686(91)80022-C

45. Mishchuk N. A. Concentration polarization of interface and non-linear electrokinetic phenomena. *Advances in Colloid and Interface Science*. 2010;160(1-2): 16–39. https://doi.org/10.1016/j.cis.2010.07.001

46. Rubinstein I., Zaltzman B. Electro-osmotically induced convection at a permselective membrane. *Physical Review E*. 2000;62(2): 2238. https://doi.org/10.1103/PhysRevE.62.22381

47. Zaltzman B., Rubinstein I. Electro-osmotic slip and electroconvective instability. *Journal of Fluid Mechanics*. 2007;579: 173–226. https://doi.org/10.1017/S0022112007004880

48. Helfferich F. G. *Ion exchange*. Courier Corporation; 1995.

49. Zabolotskii V.I., Lebedev K.A., Sheldeshov N.V. Ion-transfer across a membrane in the presence of a preceding slow homogeneous chemical reaction in the diffusion layer. *Russian Journal of Electrochemistry*. 2017;53(9): 1083–1097. https://doi.org/10.7868/S0424857017090079

50. Sharafan M. V., Gorobchenko A.D., Nikonenko V.V. Effect of acetic acid dissociation reaction on the limiting current density in a system with a rotating membrane disk. *Membranes and Membrane Technologies*, 2024;6(4): 290–297. In press.

51. Martí-Calatayud M. C., Ruiz-García M., Pérez-Herranz V. On the selective transport of mixtures of organic and inorganic anions through anion-exchange membranes: A case study about the separation of nitrates and citric acid by electrodialysis. *Separation and Purification Technology*. 2025;354: 128951. https://doi.org/10.1016/j.seppur.2024.128951

52. Anion exchange membranes. Available at: https://www.astom-corp.jp/en/product/10.html

Information about the authors

Olesya A. Yurchenko, Cand. Sci. (Chem.), Junior Research Fellow, Department of Physical Chemistry, Kuban State University (Krasnodar, Russian Federation).

https://orcid.org/0000-0001-5623-8657

olesia93rus@mail.ru

Ksenia V. Solonchenko, postgraduate student, Engineer, Department of Physical Chemistry, Kuban State University (Krasnodar, Russian Federation).

https://orcid.org/0009-0005-8152-7879

sol.ksenia17@yandex.ru

Natalia D. Pismenskaya, Dr. Sci. (Chem.), Professor at the Department of Physical Chemistry, Kuban State University (Krasnodar, Russian Federation).

https://orcid.org/0000-0001-5736-0136

n_pismen@mail.ru

Received October 28, 2024; accepted after reviewing November 8, 2024; accepted for publication November 15, 2024; published online September 25, 2025.